

Article

New Biological Activities of *Lythrum salicaria* L.: Effects on Keratinocytes, Reconstructed Epidermis and Reconstructed Skins, Applications in Dermo-Cosmetic Sciences

Glorianne Jouravel ^{1,3}, Samuel Guénin ² , François-Xavier Bernard ², Claire Elfakir ³, Philippe Bernard ¹ and Franck Himbert ^{1,*}

¹ GREENPHARMA SAS, 3 Allée du Titane, 45100 Orléans, France; philippe.bernard@greenpharma.com

² BIOalternatives SAS, 1 bis Rue des Plantes, 86160 Gençay, France; s.guenin@bioalternatives.com (S.G.); fx.bernard@bioalternatives.com (F.-X.B.)

³ ICOA (Institut de Chimie Organique et Analytique), Université d'Orléans, CNRS, UMR 7311, Rue de Chartres, F-45067, 45100 Orléans, France; glorianne.jouravel@etu.univ-orleans.fr (G.J.); claire.elfakir@univ-orleans.fr (C.E.)

* Correspondence: franck.himbert@greenpharma.com; Tel.: +33-238-259-980

Received: 23 October 2017; Accepted: 21 November 2017; Published: 25 November 2017

Abstract: The perennial and widespread herb *Lythrum salicaria* L., also called purple loosestrife, is a plant that is traditionally used in European medicine. Purple loosestrife is known for its ability to treat internal disorders, such as gastrointestinal issues or hemorrhages. Our objective was to take another look on this natural source of ellagitannins in terms of biological activities. Exploration of the phytochemical content of an extract of aerial parts of *Lythrum salicaria* L. was completed before initiating research on its biological effects towards keratinocytes, reconstructed epidermis, and skins. The potential of the natural compounds were evaluated by topical treatment of reconstructed tissues. The extract and one of its major compounds were able to act as pro-differentiating and protecting agents towards skin cells by stimulating the expressions of markers taking part in the structure of epidermis and dermis. Also, the extract showed beneficial effects on the global morphology of the skin. Thus, *Lythrum salicaria* L. constitutes a new natural source for the development of active ingredients for the dermo-cosmetic field.

Keywords: *Lythrum salicaria* L.; purple loosestrife; natural extract; vescalagin; skin barrier function; epidermis; differentiation; TGK; 3D model

1. Introduction

Belonging to the Lythraceae family, *Lythrum salicaria* L. (or Purple loosestrife) is an herbaceous perennial plant that is quite easily recognizable with its flowering parts displaying small purple flowers. *Lythri herba* is widely distributed in Europe, North America, and Asia, and grows in wet places. *Lythrum salicaria* L. is known as a medicinal plant that was used in the ancient times. Naturalists and pharmacologists of the Greco-Roman period already reported its medicinal properties [1], and nowadays the plant is registered in European Pharmacopoeia. It has traditionally been employed as a strong astringent and haemostatic agent to treat gastrointestinal tract ailments, such as dysentery or diarrhea [2]. In terms of composition, studies reported polyphenols and heteropolysaccharides as principal phytochemical families [1]. *Lythrum salicaria* L. is a rich source of polyphenols and mainly of ellagitannins, a class of hydrolysable tannins [3]. In this way, the total tannin content is a means of characterization of this herb according to its pharmacopoeial monograph. Polyphenols are natural active compounds that are able to display anti-aging effects as they have strong antioxidant activity [4].

More generally, botanicals possess various effects and display several activities simultaneously [5]. Thus, any of them could be considered in their capacity to cope with many different health issues. Moreover, since ancient times, botanical ingredients have been used as remedies and care products and still play an important role in contemporary cosmetics by being highly efficient [4]. Purple loosestrife—as a native plant in France, widespread and perennial—constituted a sustainable material to initiate a new and modern exploration of its potential. Based on previous knowledge notably about its composition, which suggested the potential of *Lythri herba*, the objective of our work was to innovate by searching a new application of a *Lythrum salicaria* extract, and more specifically by looking for a beneficial effect for skin physiology.

Skin is a complex system organized as a stratified cellular epidermis lying on a dermal connective tissue (dermis and hypodermis). Epidermis is composed of layers of keratinocytes that are constantly renewed thanks to proliferation and differentiation with an increasing differentiation state from the basal layer (with the less differentiated cells) to the *stratum corneum* (top of the epidermis, the most differentiated state) [6,7]. In each layer, specific proteins are expressed and characterize differentiated epidermis, such as cytokeratins (keratins 5, 14, 1, 10, etc.), late differentiation markers (transglutaminase M1 (TGK), filaggrin), and proteins of the cornified envelope (involucrin, small proline rich proteins). These cells migrate and ultimately differentiate into corneocytes that form the cornified layer at the surface of the skin. Before becoming corneocytes, the keratinocytes produce proteins and lipids to form a water-impermeable barrier, the *stratum corneum* [8,9]. Skin needs to be stable, while at the same time retaining dynamics to allow for tissue regeneration and response to cutaneous injuries [6,7,10]. One of the essential functions of skin is to constitute a protective barrier to avoid the loss of inner fluids and to prevent the entry of external aggressive agents [11]. Indeed, skin has to face daily environmental aggressions, such as ultraviolet radiation from the sun [12], air pollution or irritations, and wounds. At the same time, a protective barrier but a fragile organ (not thicker than a few millimeters), skin has the faculty to renew itself constantly. Regeneration allows for repairing damages and replacing old cells. Nevertheless, skin cannot escape aging [12,13]. Aging involves dramatical changes in the structure, functioning, and appearance of the skin, such as thinning of the epidermis, degradation of the extracellular matrix (ECM), loss of capacity of regeneration or wound healing, elastosis, and the formation of wrinkles [4,13]. This protective function of the skin is essentially performed by the *stratum corneum* [8,9].

One way to maintain epidermal integrity and more generally to prevent or at least limit the inevitable phenomenon of skin-aging is the use of topical treatments based on natural active ingredients [14]. Therefore, the goal of the present work was to take another look at *Lythrum salicaria* L. by investigating again its metabolite content and its biological activities to highlight its potential interest in skin homeostasis and in the dermo-cosmetic field.

2. Materials and Methods

2.1. Plant Material

Aerial parts of *Lythrum salicaria* L. were collected during the flowering period in summer 2012, in the department of Cher in Region Centre-Val de Loire in France, and were identified by Patrice André, botanical expert (Botanicosm'ethic). A voucher specimen of *Lythrum salicaria* L. has been deposited at the herbarium of Greenpharma under the individual number P2759998P.

2.2. Hydro-Alcoholic Extraction

Air-dried aerial parts of *Lythrum salicaria* L. were crushed and then extracted with ethanol-water in the proportion of 30:70 (*v:v*) for 24 h under stirring and away from light. The plant-solvent ratio was 1 to 10 (*w:v*). After 24 h, the mixture was successively filtered by decreasing size-pore membranes to a filtration on glass fiber with porosity of 1 μ m. The filtrate was treated with active carbon for

30 min under stirring. Finally, the dry extract was obtained after a 1 μm pore-size glass fiber filtration, evaporation of ethanol under vacuum, and freeze-drying.

2.3. Characterization of Major Compounds

2.3.1. Isolation

Isolation of the two main compounds was conducted on semi-preparative HPLC by injecting a solution of the extract of *Lythrum salicaria* L. The solution was obtained after a solubilization of the extract in a mixture of water/methanol 80:20 (*v:v*) with 0.5% formic acid and passed through a SPE-C18 cartridge (Phenomenex, Le Pecq, France). The eluted solution was concentrated by evaporation of methanol and a part of water under vacuum. The final concentration of dry matter was estimated to 61.5 $\text{mg}\cdot\text{mL}^{-1}$. Mobile phases A and B were water with 0.5% formic acid and methanol with 0.1% formic acid, respectively. The separation was carried out at 30 °C on a column Synergi Fusion-RP of 250 mm \times 10 mm; 4 μm (Phenomenex, Le Pecq, France) with a gradient elution programmed at a flow rate of 4.0 $\text{mL}\cdot\text{min}^{-1}$. The following multi-step linear gradient with different proportion of mobile phase B was applied: 0 min, 0% B; 15 min, 10% B; 23.5 min, 10% B; 26 min, 70% B; 31 min, 70% B. The volume per injection was 0.8 mL and the UV detector was set to 345 nm. This wavelength of absorbance was chosen after an adjustment to avoid the UV signal to be saturated due to the high concentration of the injected solution. Each chromatographic peak was collected and at the end of all the injections, and each fraction was dried by evaporation under vacuum and freeze-drying.

2.3.2. ESI-Q-TOF-HRMS and MS₂ Analysis

High-Resolution Mass Spectrometry (HRMS) and MS₂ analyses were conducted using a maXis Q-TOF (BrukerDaltonics, Bremen, Germany) equipped with an electrospray ionization (ESI) source through flow injection analysis (FIA) of methanolic solutions of isolated compounds. Experiments were performed in positive and negative ionisation modes using a drying gas temperature of 200 °C, a drying gas flow of 7.0 $\text{L}\cdot\text{min}^{-1}$, and a nebulizer gas pressure of 0.6 bar. For the positive mode, the scan range was 50–2500 m/z and the capillary voltage was set at 4.5 kV. For the negative mode, the scan range was 50–3000 m/z and the capillary voltage was at 4 kV. MS₂ experiments were manually performed in order to optimize the collision energy. Most intense singly charged ions observed in MS₁ were isolated; the isolation window width was 8 m/z . The collision energy applied to obtain the fragmentation data were, respectively, 25 eV in positive and 55 eV in negative. Data for the determination of accurate masses of MS₁ and MS₂ ions were processed with Data Analysis 4.4 and possible elemental formulae were determined using the SmartFormula algorithm.

2.3.3. NMR Analysis

¹H and ¹³C-Nuclear Magnetic Resonance (NMR) spectra were recorded on Bruker Avance II NMR instrument (BrukerDaltonics, Billerica, MA, USA). The experiments were performed at 298.1K, using acetone-d₆ and acetone-d₆ + deuterated water, respectively, for ¹H NMR (400 MHz) and ¹³C NMR (100 MHz). Chemical shifts (δ) are given in ppm and coupling constants (J) are given in Hz.

2.3.4. Content in Major Compounds

The rate of the major compounds that were identified in the extract was evaluated through quantification by HPLC-UV using vescalagin (Sigma-Aldrich, Saint-Quentin Fallavier, France) as standard. Surface areas of vescalagin in standard solutions or in the extract are measured at 235 nm, which is the wavelength of maximum absorbance of vescalagin. Standard solutions were dissolved in water/methanol in proportion 50:50 (*v:v*). The extract was dissolved in the same solvent and centrifuged for 5 min at 18 000 rcf. HPLC column was a Synergi Polar-RP of 150 mm \times 4.6 mm, 4 μm (Phenomenex, Le Pecq, France). Mobile phases A and B were water with 0.1% formic acid and methanol with 0.1% formic acid, respectively. The separation was carried out at 30 °C with a gradient

elution programmed at a flow rate of $1.0 \text{ mL}\cdot\text{min}^{-1}$. The following multi-step linear gradient with different proportion of mobile phase B was applied: 0 min, 0% B; 5 min, 0% B; 22 min, 13% B; 23 min, 70% B; 33 min, 70% B.

2.4. Biological Activity

2.4.1. Monolayer of Keratinocytes Culture and Treatments

Normal human epidermal keratinocytes (NHEK) were obtained as previously described [15,16]. The cells were seeded in 96 well-plates and grown into confluence. Then they were treated or not (control) with the *Lythrum salicaria* extract (concentrations indicated in the legends of the figures) or CaCl_2 at 1.5 mM and were incubated during various times depending on the endpoint: 24 h (gene expression), 72 h (filaggrin and TGK expression) or 96 h (KRT10 expression). Experiments were performed in triplicate.

2.4.2. Reconstructed Human Epidermis Culture and Treatments

Reconstructed human epidermis (RHE) was generated on polycarbonate culture inserts, from surgical samples of pediatric foreskins, as previously described [15,16]. After shifting to air/liquid interface, RHE were cultured for seven days in the presence or not (control, no Vitamin C) of the *Lythrum salicaria* extract (concentrations indicated in the legends of the figures) or of Vitamin C. RHE treatments were renewed every two or three days. Experiments were performed in triplicate.

2.4.3. Full Thickness Reconstructed Skins Culture and Treatments

A skin model was composed of keratinocytes seeding on a collagen layer containing fibroblasts and cultivated at the interface air/liquid to obtain a full thickness reconstructed skin (FTSK). Dermis-equivalent was prepared by mixing a rat tail collagen solution to fibroblast suspension ($1.3 \text{ mg}\cdot\text{mL}^{-1}$ and 0.5×10^6 cells/mL, final concentration/content, in a volume of $400 \mu\text{L}$ /insert). After 2 h polymerization/solidification, epidermal cell suspension was added and the FTSK were incubated in complete Epilife medium (Cascade Biologics, Portland, OR, USA), supplemented by $5 \mu\text{g}\cdot\text{mL}^{-1}$ insulin and 1.5 mM CaCl_2 for two days. The inserts were then placed at the interface air-medium on sterile gauze. Untreated FTSK were incubated in complete Epilife medium (supplemented with $5 \mu\text{g}\cdot\text{mL}^{-1}$ insulin and 1.5 mM CaCl_2 , $50 \mu\text{g}\cdot\text{mL}^{-1}$ vitamin C and $3 \text{ ng}\cdot\text{mL}^{-1}$ KGF). For depleted conditions, FTSK were cultivated in depleted medium consisting in Epilife medium supplemented without some complements and containing or not (untreated depleted FTSK) the test compounds (concentrations indicated in the legends of the figures). All of the FTSK conditions were then incubated for nine days with medium and treatments renewal every two or three days. All of the experimental conditions were performed in quadruplicate.

2.4.4. Expression of Genes Monitored by RT-qPCR Array

NHEK total RNA were isolated using NucleoSpin RNA II kit (Macherey-Nagel, Duren, Germany) and reverse-transcribed with SuperScript II Reverse Transcriptase (Invitrogen Life Technologies, Thermo Fisher Scientific, Waltham, MA, USA), according to the manufacturer's instructions. Quantitative real time PCR was carried out using the LightCycler-FastStart DNA MasterPlus SYBR Green I kit on LightCycler 480 (Roche Diagnostics, Meylan, France). The reaction components were 1X DNA Master Mix, and $0.5 \mu\text{M}$ of HPLC purified sense and anti-sense oligonucleotides purchased from Eurogentec (Eurogentec France, Angers, France), designed using Primer3 software. Gene expression in cells was normalized to GAPDH housekeeping gene and reported according to the $\Delta\Delta\text{C}_T$ method as RNA fold increase: $2^{\Delta\Delta\text{C}_T} = 2^{\Delta\text{C}_T \text{ sample} - \Delta\text{C}_T \text{ reference}}$.

2.4.5. Immunofluorescence

At the end of the treatment, NHEK monolayers were rinsed with PBS and fixed. The cells were incubated with anti-KRT10 (SC-23877, SantaCruz Biotechnology, Heidelberg, Germany), anti-FLG (SC-66192, SantaCruz Biotechnology, Heidelberg, Germany) or anti-TGK (0175003, Tebubio, Le Perray-en-Yvelines, France) antibody. Goat-anti mouse labeled with Alexa Fluor[®]488 was used as a secondary antibody and the cell nuclei were stained with Hoechst 33258. Images were captured using an INCell Analyzer[™] 1000 (GE Healthcare, Aulnay-sous-Bois, France) and were processed with Developer Toolbox 1.5 software (GE Healthcare).

2.4.6. ELISA Tests

The cell culture supernatants from each condition were collected and stored at $-20\text{ }^{\circ}\text{C}$ until analysis. ELISA quantification of MMP-1 (R&D Systems, Lille, France), MMP-3 (R&D Systems, Lille, France) and procollagen I (Takara, Saint-Germain-en-Laye, France) release was performed following supplier's recommendation.

2.4.7. Histological Analysis

At the end of incubation, FTSK were fixed with formaldehyde solution, dehydrated in multiple baths with increasing concentration of ethanol, and then embedded in paraffin. Transversal sections were performed with a microtome ($5\text{ }\mu\text{m}$ thickness). Then, the sections were deparaffinized and stained with hematoxylin, eosin and safran solution. After being mounted in "CV Ultra Mounting Medium", the sections were observed using a NIKON E400 microscope (objective lens $\times 40$). The images were recorded with a NIKON DS-Ri1 camera (Nikon Instruments Inc., Melville, NY, USA) and NIS-Elements 4.13.04 software (Nikon Instruments Inc., Melville, NY, USA). For each condition, two representative images were presented, as well as one mosaic image of one FTSK.

RHE were processed, as previously described [15]. Briefly, at the end of incubation they were fixed with formaldehyde and fixed tissues were dehydrated with increasing ethanol concentrations, embedded in paraffin, and sections were carried out using a microtome (thickness of $5\text{ }\mu\text{m}$). The sections were deparaffinised, washed, and incubated with hydrogen peroxide for endogenous peroxidase inhibition. The sections were incubated with anti-KRT10, anti-FLG, or anti-TGK antibody, and then detected using a biotin-conjugated secondary antibody (Dako, Kit LSAB+, K0690, Agilent Technologies, Santa Clara, CA, USA). After peroxidase-conjugated streptavidin (Dako, Kit LSAB+, K0690) and peroxidase substrate addition (Dako, Substrate hyper-sensitive AEC+), nuclei were counter-stained using a solution of haematoxylin. Sections were observed using a NIKON E400 microscope. The images were captured using a NIKON DS-Ri1 and processed with NIS-Elements 3.10 software. One representative picture of each experimental condition was presented.

2.4.8. Statistical Analysis

All of the results are expressed as mean \pm standard deviation. The inter-group comparisons were performed by an unpaired Student's t-test. Results were considered as significant when $p < 0.05$.

3. Results

3.1. Extraction, Isolation, Structure Determination and Quantification of Major Compounds

A dry hydro-ethanolic extract was obtained by maceration. In the following text, this extract will be cited as *Lythrum salicaria* extract (*Lyth. s* extract) or purple loosestrife extract.

The two major compounds of the hydro-ethanolic extract of *Lythrum salicaria* L. presented a UV maximum at 235 nm. They were isolated with a level of purity of 97% minimum and had an appearance of off-white amorphous powders.

Table 1. High-Resolution Mass Spectrometry (HRMS) and MS₂ data for compound **1** and compound **2** determined by ESI-Q-TOF analyses (HHDP, hexahydroxydiphenoyl unit = 302.0057 g·mol⁻¹). Ions with *m/z* in **bold** were isolated for fragmentation experiments in MS₂. MS₂ ions without attribution were all singly charged ions.

Compound	<i>m/z</i> +	Molecular Formula	Error (ppm)	MS ₂	Molecular Formula	<i>m/z</i> −	Molecular Formula	Error (ppm)	MS ₂	Molecular Formula
1	935.0783 (100) [M+H] ⁺ 952.1050 (32) [M+NH ₄] ⁺	C ₄₁ H ₂₇ O ₂₆ C ₄₁ H ₃₀ O ₂₆ N	0.3 0.1	935.0784 (71) [M+H] ⁺	C ₄₁ H ₂₇ O ₂₆	933.0630 (47) [M-H] [−] 477.0189 (10) [M-3H+Na] ^{2−} 466.0282 (100) [M-2H] ^{2−} 300.9989 (8) [HHDP-H] [−]	C ₄₁ H ₂₅ O ₂₆ C ₄₁ H ₂₃ NaO ₂₆ C ₄₁ H ₂₄ O ₂₆ C ₁₄ H ₅ O ₈	1.0 0.9 0.4 0.3	933.0635 (57) [M-H] [−]	C ₄₁ H ₂₅ O ₂₆
				917.0671 (18) [M-H ₂ O+H] ⁺	C ₄₁ H ₂₅ O ₂₅				915.0521 (27) [M-H ₂ O-H] [−]	C ₄₁ H ₂₃ O ₂₅
				873.0776 (9) [M-CO ₂ -H ₂ O+H] ⁺	C ₄₀ H ₂₅ O ₂₃				897.0449 (5) [M-2H ₂ O-H] [−]	C ₄₁ H ₂₁ O ₂₄
				633.0719 (100) [M-HHDP+H] ⁺	C ₂₇ H ₂₁ O ₁₈				889.0733 (9) [M-CO ₂ -H] [−]	C ₄₀ H ₂₅ O ₂₄
				615.0616 (75) [M-HHDP-H ₂ O+H] ⁺	C ₂₇ H ₁₉ O ₁₇				871.0653 (13) [M-CO ₂ -H ₂ O-H] [−]	C ₄₀ H ₂₃ O ₂₃
				597.0511 (24) [M-HHDP-2H ₂ O+H] ⁺	C ₂₇ H ₁₇ O ₁₆				613.0471 (16) [M-HHDP-H ₂ O-H] [−]	C ₂₇ H ₁₇ O ₁₇
				553.0608 (33) [M-HHDP-2H ₂ O-CO ₂ +H] ⁺	C ₂₆ H ₁₇ O ₁₄				569.0574 (34) [M-HHDP-CO ₂ -H ₂ O-H] [−]	C ₂₆ H ₁₇ O ₁₅
				535.0506 (66) [M-HHDP-3H ₂ O-CO ₂ +H] ⁺	C ₂₆ H ₁₅ O ₁₃				493.0052 (92)	C ₂₃ H ₉ O ₁₃
				523.0507 (17)	C ₂₅ H ₁₅ O ₁₃				489.0463 (32)	C ₂₅ H ₁₃ O ₁₁
				517.0400 (23) [M-HHDP-4H ₂ O-CO ₂ +H] ⁺	C ₂₆ H ₁₃ O ₁₂				467.0254 (89)	C ₂₂ H ₁₁ O ₁₂
				505.0400 (50)	C ₂₅ H ₁₃ O ₁₂				425.0150 (26)	C ₂₀ H ₉ O ₁₁
				495.0193 (43)	C ₂₃ H ₁₁ O ₁₃				300.9992 (100) [HHDP-H] [−]	C ₁₄ H ₅ O ₈
				469.0399 (42)	C ₂₂ H ₁₃ O ₁₂				275.0192 (40)	C ₁₃ H ₇ O ₇
				303.0137 (14) [HHDP+H] ⁺	C ₁₄ H ₇ O ₈				249.0404 (54)	C ₁₂ H ₉ O ₆
				277.0343 (16)	C ₁₃ H ₉ O ₇					
				2	935.0783 (100) [M+H] ⁺ 952.1049 (40) [M+NH ₄] ⁺				C ₄₁ H ₂₇ O ₂₆ C ₄₁ H ₃₀ O ₂₆ N	0.3 0.2
917.0677 (7) [M-H ₂ O+H] ⁺	C ₄₁ H ₂₅ O ₂₅	915.0514 (17) [M-H ₂ O-H] [−]	C ₄₁ H ₂₃ O ₂₅							
873.0781 (10) [M-CO ₂ -H ₂ O+H] ⁺	C ₄₀ H ₂₅ O ₂₃	889.0757 (12) [M-CO ₂ -H] [−]	C ₄₀ H ₂₅ O ₂₄							
633.0721 (68) [M-HHDP+H] ⁺	C ₂₇ H ₂₁ O ₁₈	871.0619 (9) [M-CO ₂ -H ₂ O-H] [−]	C ₄₀ H ₂₃ O ₂₃							
615.0615 (40) [M-HHDP-H ₂ O+H] ⁺	C ₂₇ H ₁₉ O ₁₇	631.0574 (64) [M-HHDP-H] [−]	C ₂₇ H ₁₉ O ₁₈							
597.0511 (20) [M-HHDP-2H ₂ O+H] ⁺	C ₂₇ H ₁₇ O ₁₆	569.0576 (41) [M-HHDP-CO ₂ -H ₂ O-H] [−]	C ₂₆ H ₁₇ O ₁₅							
553.0612 (26) [M-HHDP-2H ₂ O-CO ₂ +H] ⁺	C ₂₆ H ₁₇ O ₁₄	467.0257 (32)	C ₂₂ H ₁₁ O ₁₂							
535.0506 (34) [M-HHDP-3H ₂ O-CO ₂ +H] ⁺	C ₂₆ H ₁₅ O ₁₃	425.0150 (74)	C ₂₀ H ₉ O ₁₁							
523.0503 (12)	C ₂₅ H ₁₅ O ₁₃	300.9990 (99)	C ₁₄ H ₅ O ₈							
517.0402 (10) [M-HHDP-4H ₂ O-CO ₂ +H] ⁺	C ₂₆ H ₁₃ O ₁₂	275.0199 (33)	C ₁₃ H ₇ O ₇							
505.0400 (16)	C ₂₅ H ₁₃ O ₁₂	249.0407 (28)	C ₁₂ H ₉ O ₆							
495.0195 (81)	C ₂₃ H ₁₁ O ₁₃									
469.0402 (100)	C ₂₂ H ₁₃ O ₁₂									
439.0295 (14)	C ₂₁ H ₁₁ O ₁₁									
303.0136 (8) [HHDP+H] ⁺	C ₁₄ H ₇ O ₈									
277.0343 (10)	C ₁₃ H ₉ O ₇									

Analyses in HRMS were conducted to detect the accurate masses of molecular ions and obtain the molecular formulae. Fragmentation of the compounds was also registered. HRMS and MS₂ data are detailed in Table 1. The two major compounds (1 and 2) provided comparable signals: m/z 935.078 for $[M+H]^+$, m/z 952.105 for $[M+NH_4]^+$, m/z 933.063 for $[M-H]^-$ and m/z 466.028 $[M-2H]^{2-}$ were detected. Also, a slightly unusual form of ion was detected with m/z 477.019 attributed to $[M-3H+Na]^-$ according to the suggested formula. The neutral molecular formula was determined to be C₄₁H₂₆O₂₆ corresponding to a monoisotopic mass of 934.0712 g·mol⁻¹. Based on the literature of the studied plant, this information indicated two isomers of the class of ellagitannins: vescalagin and castalagin [3,17]. The structures of these ellagitannins are presented in Figure 1.

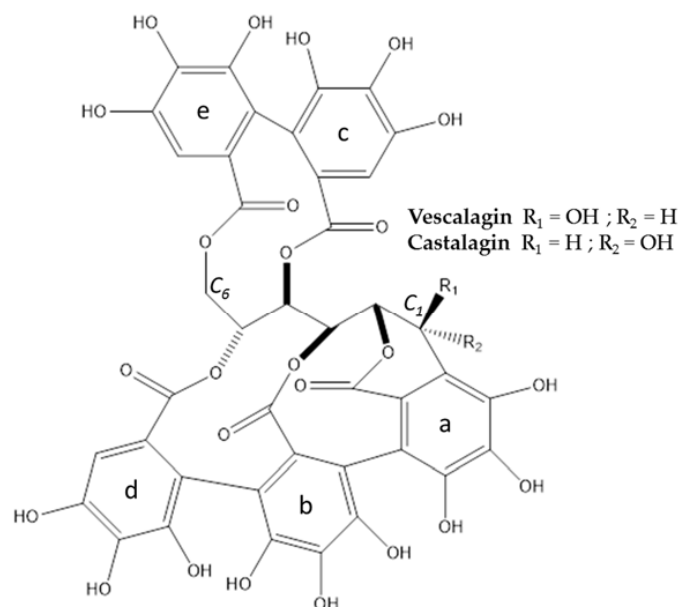


Figure 1. Structure of vescalagin (1) and castalagin (2).

Compounds 1 and 2 were observed in both negative and positive ionisation modes. In positive mode, singly charged ions were predominant, whereas in negative mode, doubly charged ions were the most intense. Regarding the fragmentation patterns, neutral losses of water and/or carbon dioxide were recovered and were consistent with the hypothesis of structures (presence of hydroxy and ester functions on the ellagitannins). Moreover, characteristic ions for ellagitannins were observed, such as the neutral loss of a hexahydroxyphenoyl (HHDP) group with the observed m/z 633.072 (+)/631.057 (−), or the HHDP group itself with the m/z 303.014 (+)/300.999 (−).

To confirm the hypotheses and to distinguish compound 1 from compound 2, they were analyzed by ¹³C-NMR and ¹H-NMR experiments. The assignment of sugar and aromatic protons and carbons was achieved based on one dimensional NMR experiments (see Table 2).

Based on HRMS and literature, we supposed that the two compounds were the epimers vescalagin and castalagin. The literature indicated that the chemical shift and the coupling constant of the anomeric proton signal were different between the pair of isomers. Vescalagin has a coupling constant equal or less than 2 Hz because the anomeric proton is in the beta orientation, whereas for castalagin, the coupling constant is larger. In our experiments, for compound 1, a chemical shift of 4.87 ppm and a coupling constant was 2.00 Hz indicated the beta orientation of the hydroxyl group at the C₁ of the sugar moiety [18]. On the contrary, for compound 2, a chemical shift of 5.71 ppm and a coupling constant of the anomeric proton signal larger than the one of compound 1 (coupling constant of 4.40 Hz) for the proton H₁ indicated the alpha orientation of the hydroxyl group at the C₁ of the sugar moiety [18]. Moreover, all of the NMR data collected for compounds 1 and 2 were consistent with data presented in literature for vescalagin and castalagin, respectively [3,19].

Table 2. ^1H and ^{13}C -NMR data (at, respectively, 400 and 100 MHz) for compound 1 and compound 2; chemical shifts (δ) are expressed in ppm and coupling constant (J) in Hz.

Type of Protons and/or Carbons	Position	Compound 1		Compound 2	
		δ_{C}	δ_{H}	δ_{C}	δ_{H}
Glycosyl	1	65.37	4.87 (d; 2.00)	65.62	5.71 (d; 4.40)
	2	77.61	5.19–5.23 (m; na)	73.36	5.03–5.05 (m; na)
	3	68.29	4.56 (dd; 0.80/6.80)	66.38	5.03–5.05 (m; na)
	4	69.17	5.19–5.23 (m; na)	68.51	5.25 (t; 7.20)
	5	71.03	5.65 (d; 6.40)	70.50	5.62 (dd; 1.60/8.00)
	6	77.61	5.08 (dd; 2.80)	64.65	5.11 (dd; 2.40/12.80)
	6'		4.01 (d; 12.80)		4.00 (d; 12.80)
Aromatic	H _{ar} (c)		6.77 (s; na)		6.81 (s; na)
	H _{ar} (d)		6.76 (s; na)		6.78 (s; na)
	H _{ar} (e)		6.61 (s; na)		6.63 (s; na)
	C=O (a)	165.37		164.04	
	C=O (b)	165.49		164.98	
	C=O (c)	166.50		165.99	
	C=O (d)	167.23		166.55	
C=O (e)	169.27		168.58		

The two major compounds of the extract of aerial parts of *Lythrum salicaria* L. are vescalagin (1) and castalagin (2). They were quantified respectively at 4.6% and 2.6% in the dry extract.

3.2. Cytotoxicity

Assays to study biological effects of both the extract of *Lythrum salicaria* L. and vescalagin were performed at non-cytotoxic concentrations (concentrations selected following a MTT (MethylThiazolyldiphenyl-Tetrazolium) assay (data not shown).

3.3. Pro-Differentiation Effect of *Lythrum Salicaria* Extract

3.3.1. Levels of Expression of Genes Implicated in Differentiation

In order to identify a potential effect on epidermis differentiation, NHEK were incubated with *Lythrum salicaria* L. extract and the effect of this extract was evaluated at the gene expression level by RT-qPCR. As shown in Figure 2, the incubation of the cells with extract induced a strong increase in the mRNA of differentiation markers, mainly TGK, keratin 1 (KRT1) and KRT10, and to a lesser extent, filaggrin, loricrin and involucrin (from 400% to 6000% of the untreated control depending of the marker). Looking at the presence of various proteins, such as involucrin, loricrin, and filaggrin gives indications of fully differentiated epidermal keratinocytes and corneocytes [20]. These structural proteins help to maintain the cutaneous barrier. Filaggrin helps to stabilize the keratin network, which serves as a crucial scaffold for other components of the cornified layer. Indeed, involucrin and loricrin are cross-linked by TGK1 [6]. One could also note that for most of the aforementioned markers (except for involucrin), the stimulation induced by *Lythrum salicaria* L. extract was stronger than that of the well described keratinocyte differentiating agent CaCl_2 (Figure 2) [21]. Within the epidermis, at high concentration, calcium generates the differentiation of keratinocytes rather than their proliferation [13]. Specific keratins KRT1 and KRT10 were much more expressed in response to *Lythrum salicaria* extract. These keratins are markers of supra-basal layers and clearly indicate that epidermal cells are developing towards a terminal differentiation state [20]. The high levels of filaggrin and loricrin in skins treated with the extract participated to the resistance of the cornified envelope. The level of TGK was increased with the extract. It plays a major role in the assembly of components of the cornified layer.

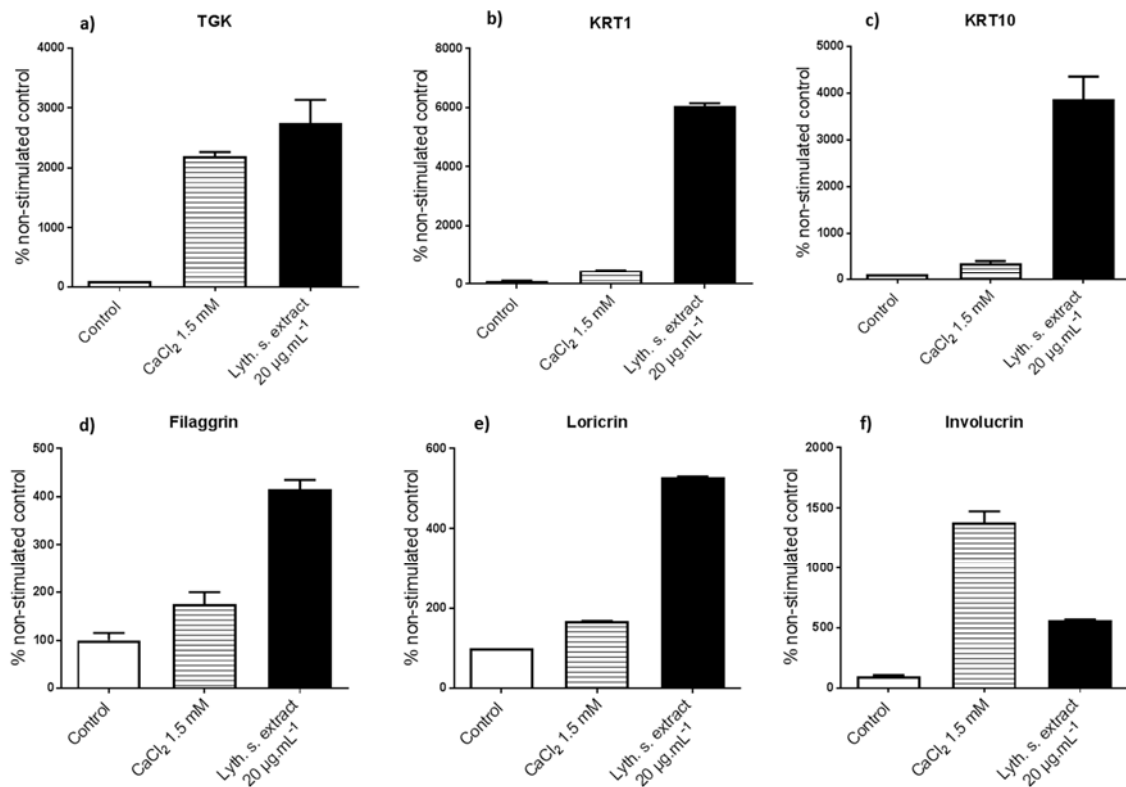


Figure 2. Effects of *Lythrum salicaria* (*Lyth. s.* extract) extract on the expression of mRNA of keratinocytes differentiation markers. Normal human epidermal keratinocytes (NHEK) were treated for 48 h with CaCl₂ at 1.5 mM, *Lyth. s.* extract at 20 µg·mL⁻¹ and mRNA levels were evaluated by RT-qPCR: (a) transglutaminase M1 (TGK); (b) keratin 1 (KRT1); (c) KRT10; (d) Filaggrin; (e) Loricrin; (f) Involucrin. Results are from one representative experiment.

We observed significant stimulations of the expression of keratinocyte genes that are involved in differentiation and structuration of the complexity of the epidermis thanks to the treatment by *Lythrum salicaria* extract. At this stage, the extract turned out to be a pro-differentiating agent.

3.3.2. Expressions of Characteristic Proteins in Differentiated Keratinocytes

We then confirmed the effect of *Lythrum salicaria* extract at the protein level. Expression of TGK, KRT10, and filaggrin proteins was evaluated in NHEK by immunofluorescent staining of these proteins after 72 h of treatment (see Figure 3). The positive control condition was a treatment with CaCl₂ at 1.5 mM. The negative control consisted in untreated cells. By comparison with these conditions, the observation of the impact of a treatment by *Lythrum salicaria* extract at 20 µg·mL⁻¹ was possible.

In cells without any treatment, the proteins were weakly expressed. The expression of these proteins showed the same trend as previously observed at the mRNA level. *Lythrum salicaria* extract had a pro-differentiating effect with the same range of effect as that of calcium. Again, the *Lythrum salicaria* extract demonstrated its capability to promote the production of proteins, allowing for proper and efficient epidermis functions and the differentiation of its constitutive cells.

3.3.3. Histological Characterization of Reconstructed Human Epidermis (RHE)

In order to get deeper in the characterization of the positive effect of *Lythrum salicaria* extract on epidermis differentiation, we then turned on a three dimensional model of epidermis, consisting in reconstructed human epidermis (RHE). In this model, epidermis differentiation can be enhanced by the presence of vitamin C in the culture medium. Therefore, in order to identify a proper effect of *Lythrum salicaria* extract, it was added in the culture medium in the absence of vitamin C. Then, after

seven days of treatment, the expression of three differentiation markers KRT10, TGK, and filaggrin was analyzed by immunohistochemistry. Histological cross-sections of RHE are shown in Figure 4.

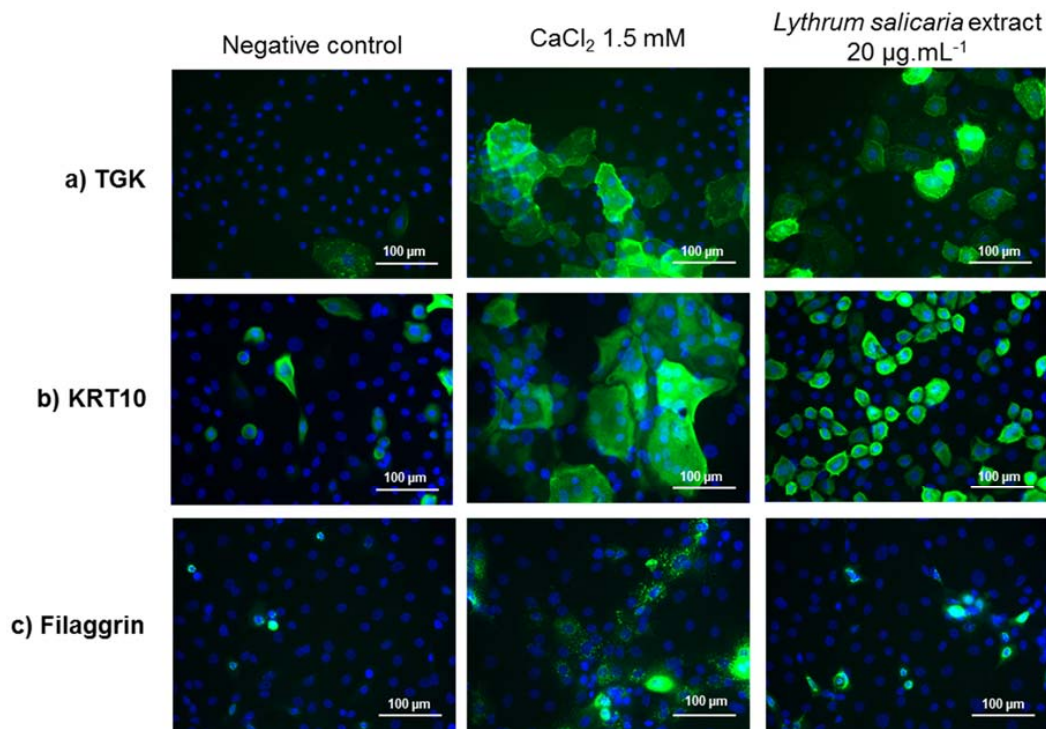


Figure 3. Immunofluorescence analysis of (a) TGK; (b) KRT10; and, (c) Filaggrin expressions in epidermal keratinocytes treated or not with CaCl_2 at 1.5 mM or *Lyth. s.* extract at $20 \mu\text{g}\cdot\text{mL}^{-1}$. After 72 h of treatment, the cells were fixed and proteins of interest were revealed using antibody directed against proteins of interest. Results are from one experiment representative of three.

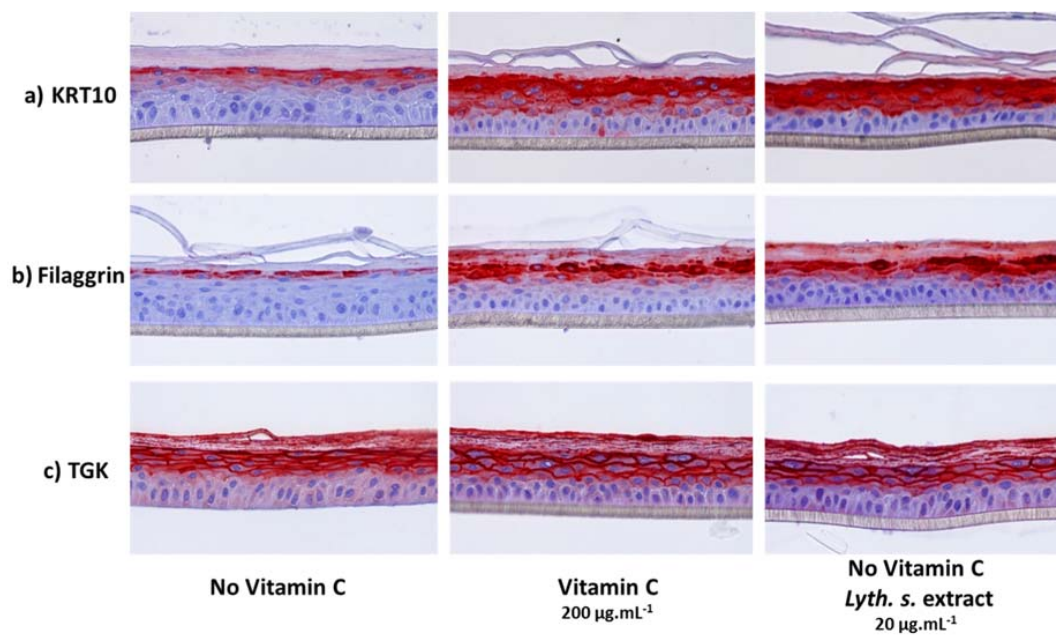


Figure 4. Effect of *Lyth. s.* extract on reconstructed human epidermis (RHE) differentiation and comparison with the effect of Vitamin C (positive control). After 7 days of treatment, the expression of the epidermis differentiation markers (a) KRT10; (b) Filaggrin; and, (c) TGK was evaluated by immunohistochemistry. Results are from one experiment representative of three.

In our study, RHE in presence of vitamin C expressed large amounts of KRT10, filaggrin, and TGK. On the contrary, the absence of vitamin C resulted in RHE with a weaker expression of the last three markers.

We noticed strong similarities of appearance between a treatment by *Lythrum salicaria* extract and vitamin C. RHE treated with the extract expressed high levels of markers, as it is showed by the intensity of the red coloration. These treated RHE were no more comparable with those that were obtained in absence of vitamin C. We could conclude that the extract had a positive effect on RHE development since it favored the differentiation of keratinocytes.

3.4. Reinforcement of the Skin

3.4.1. Skin Barrier Function Enhancement on Full Thickness Reconstructed Skin Models

Aging is characterized by a progressive loss of cohesion and architecture of the skin that is associated with an increase of a basal inflammation level, the so-called inflammaging [22]. The results that were obtained in RHE suggested that *Lythrum salicaria* extract could potentially help to reinforce aged or damaged skin. Therefore, the effect of this extract and of one of its constituents, vescalagin, was evaluated in a model of full thickness reconstructed skin (FTSK) cultivated in a depleted medium to induce an aged phenotype. Histological cross-sections of reconstructed skins are presented in Figure 5.

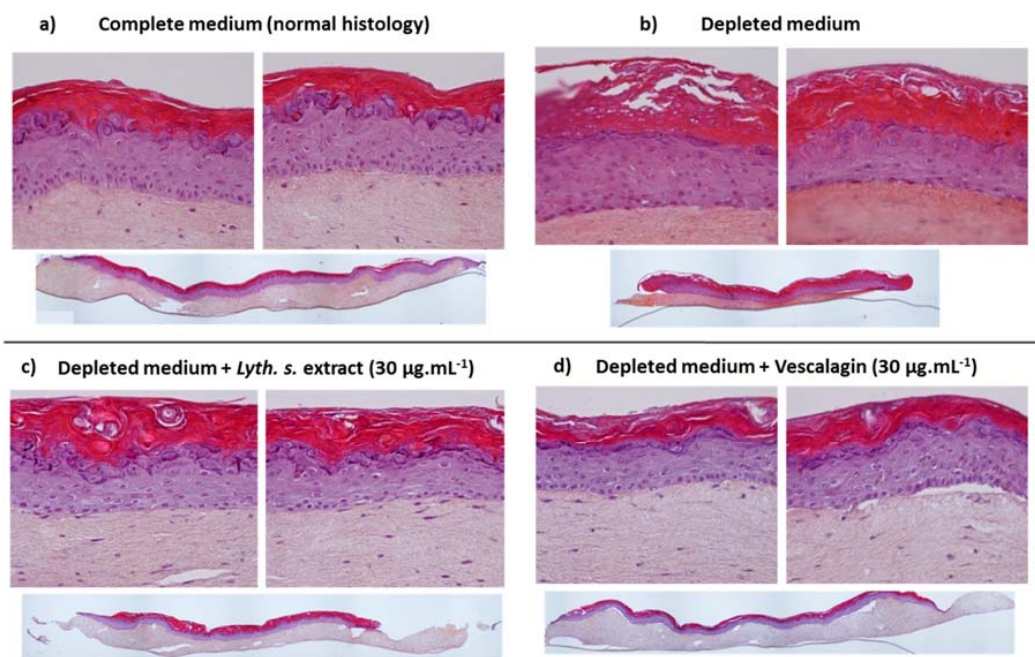


Figure 5. Evaluation of the impact of *Lyth. s.* extract and vescalagin on full thickness reconstructed skin architecture. Histological cross-sections of full thickness reconstructed skins were performed after nine days of incubation of the skin: (a) in complete medium; (b) in depleted medium; and, (c) in the presence of *Lyth. s.* extract or (d) vescalagin.

First, we checked the global appearance of control FTSK cultivated in a complete medium. These “normal” FTSK were characterized by a dermal compartment (dermal fibroblasts embedded in a collagen matrix), and an epidermal area that was composed of characteristic epidermal cell layers: a basal layer, a spinous cell layer, a granular layer, and the cornified layer (or *stratum corneum*).

In comparison with control FTSK skins described just above, aged reconstructed skins (used as control of a depleted medium of culture) presented a disorganization that was characterized by the loss

of the basal layer, a narrowing of the granular layer with decreased numbers of keratohyalin granules, a thicker *stratum corneum* and the loss of the cohesion at the dermo-epidermal junction.

The treatment of the aged reconstructed skins (cultivated in depleted medium) with the extract and vescalagin led to a global improvement of their morphology. As shown in Figure 5, they were almost similar to FTSK grown in a complete medium. Overall proportions of the three areas (dermis, epidermis, *stratum corneum*) were similar to those of normal skins. Within the epidermis, the basal and granular layers were well defined. The cohesion between the dermis and the epidermis was totally recovered with the extract, but only partially with vescalagin.

These results indicated that the molecule alone had the same properties as the extract. Indeed, when tested at the same concentrations ($30 \mu\text{g}\cdot\text{mL}^{-1}$), their activity seemed to be equivalent. A histological study of the effect of the extract or the molecule that was isolated from it showed that they were able to reinforce the skin. FTSK cultivated in depleted medium containing *Lythrum salicaria* extract or vescalagin presented an aspect that was close to that of normal skins rather than an aspect of aged skins.

3.4.2. Beneficial Effects on Extracellular Matrix

Inflammation and aging are characterized by an increased release of enzymes degrading the extracellular matrix (ECM) and a decreased content of ECM components, such as collagen I. Therefore, the levels of some metalloproteinases (MMP) in the subnatants of the FTSK were monitored by ELISA. Results are illustrated in the following graphs (see Figures 6–8). Matrix metalloproteinases (MMP) are enzymes that participate to the remodeling of the extracellular matrix. MMP-1 (Matrix metalloproteinase 1) is the predominant collagenase that degrades structural collagens, whereas MMP-3 (Matrix metalloproteinase 3) degrades collagens, proteoglycans, and matrix glycoproteins [23]. Furthermore, procollagen I, one of the major constituents of ECM, was also monitored in parallel.

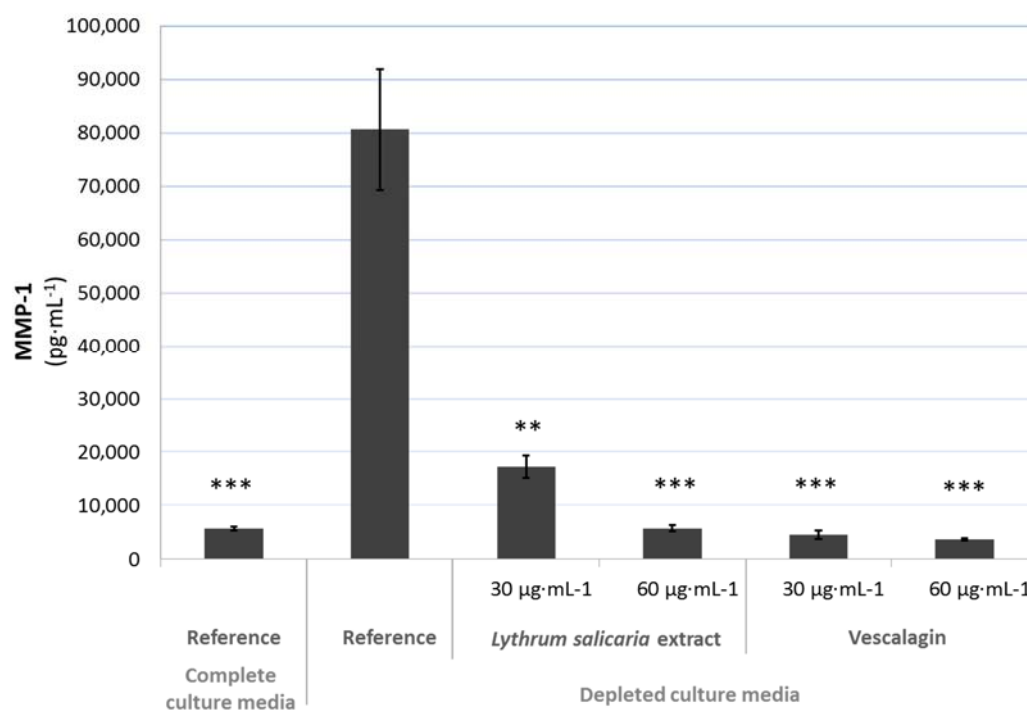


Figure 6. Effect of *Lyth. s.* extract and vescalagin on expression of MMP-1 in full thickness reconstructed skin (FTSK) monitored by ELISA quantification in cell culture subnatants of FTSK. Statistical analysis was performed *versus* the Reference condition. Statistical significances; ns: non-significant ($p > 0.05$), *: significant ($0.01 < p < 0.05$), **: very significant ($0.001 < p < 0.01$), ***: extremely significant ($p < 0.001$).

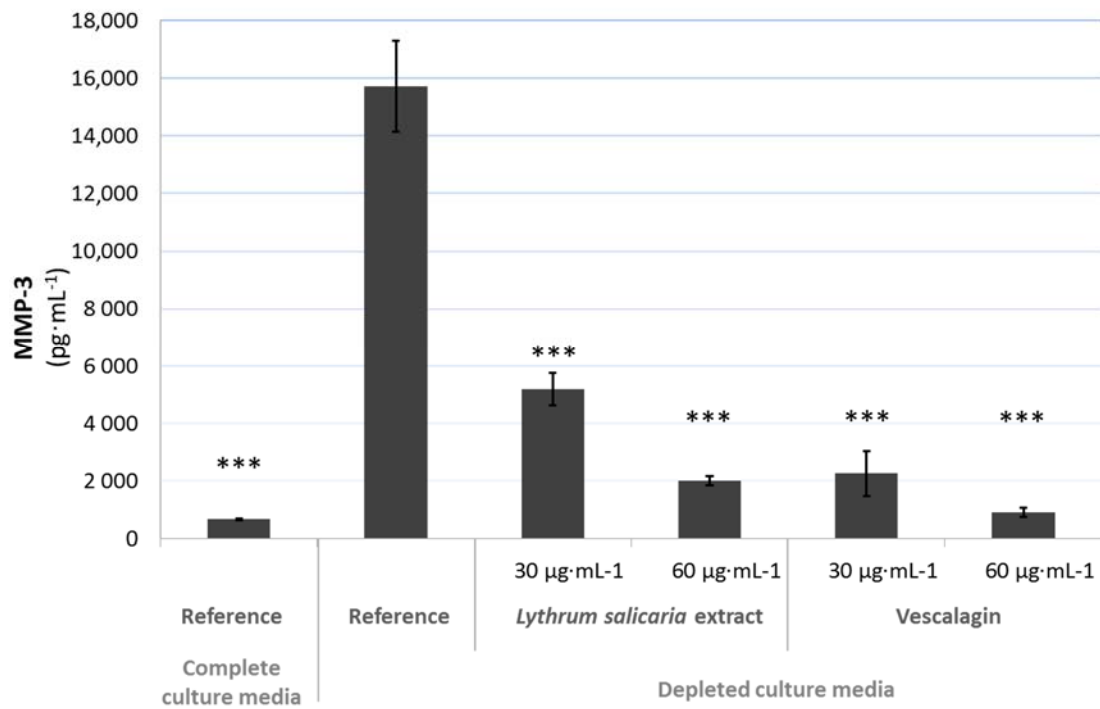


Figure 7. Effect of *Lyth. s.* extract and vescalagin on expression of MMP-3 in FTSK monitored by ELISA quantification in cell culture subnatants of FTSK (statistical significances; see details in Figure 6).

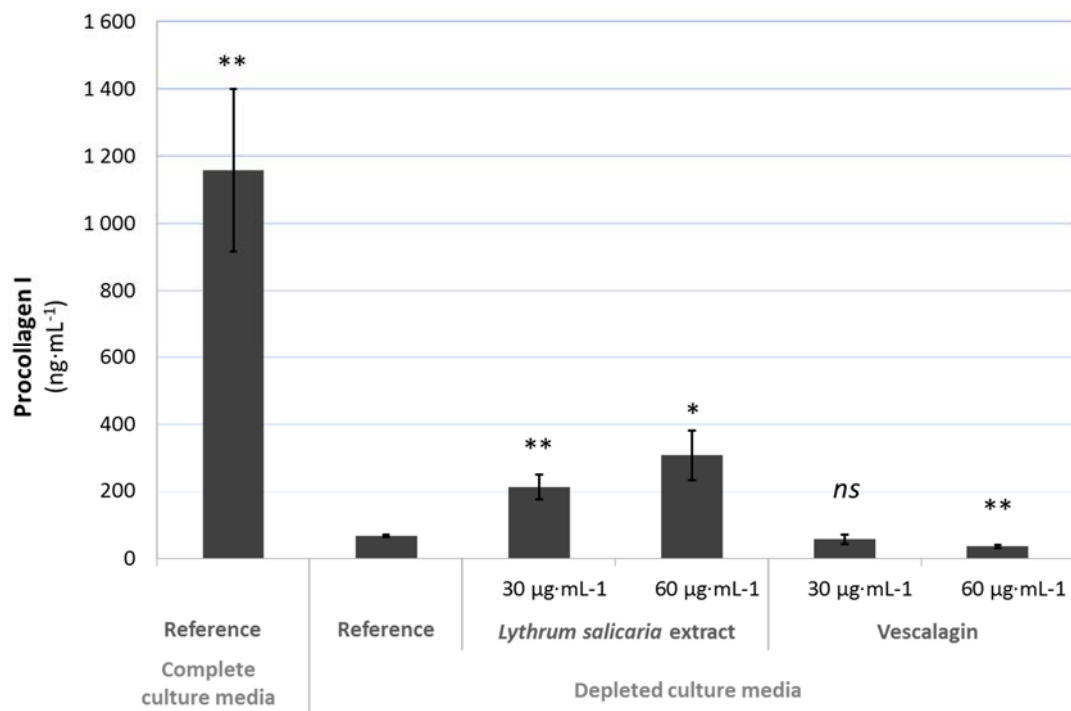


Figure 8. Effect of *Lyth. s.* extract and vescalagin on expression of procollagen I in FTSK monitored by ELISA quantification in cell culture subnatants of FTSK (statistical significances; see details in Figure 6).

As expected, in FTSK cultivated in depleted conditions, there was an increased release of MMP-1 and MMP-3 that was associated with a decreased content in procollagen I. Variations for each marker were larger than 10 fold.

The presence of both the extract and vescalagin exerted a very large decrease of expression of products that were responsible for the degradation of ECM, namely MMP-1 and MMP-3. The effect of the extract was dose-dependent (Figures 6 and 7). In parallel, an increase of procollagen I was observed, but only in response to the total extract (see Figure 8).

These elements were strong indicators of the fact that purple loosestrife extract reinforced the dermis. Treated skins were no more comparable to skins reconstructed in depleted media, but returned to a normal state.

This last experiment indicated that the products obtained from purple loosestrife acted in a favorable manner towards the dermis, which is the basement of the epidermis.

4. Discussion

In this study, the main goal was to evaluate the potential of an extract of *Lythrum salicaria* L. for beneficial effects on the skin. We focused on a hydro-alcoholic extract of aerial parts of *Lythrum salicaria* L., which was rich in ellagitannins and contained vescalagin at a rate of 4.6%. This tannin is the chemo-marker of the extract.

The biological activities of the natural products tested are associated with dermo-cosmetic applications as we tested effects towards constitutive cells of the skin through topical treatments. The *in vitro* biological tests allowed for demonstrating the effect of the skin treatment with purple loosestrife extract or one of its molecules at different scales. We monitored the effects from gene expression to skin morphology using normal human epidermal keratinocytes, reconstructed human epidermis, and full thickness reconstructed skin.

In the presence of the extract, the expression of markers of differentiation within monolayers of keratinocytes, and RHE was important. These components participate to the structuration of the cornified layer, which is essential for the skin to be protected and to maintain homeostasis. The more differentiated the epidermis is, the better defined the *stratum corneum*. This specific and outermost layer of the skin forms a skin barrier function. Not only is skin the largest organ of the human body [13], but it also has to maintain its protecting function against external aggressions. The extract was able to counteract the starving effect of a depleted medium during the development of FTSK. Skins that were treated with the extract were well structured and their morphologies were comparable to normal skins.

Vescalagin was able to generate the same effects as the extract. This molecule was able to strongly impact the morphology of FTSK, as well as to lower the quantity of MMP in aged reconstructed skins. Thus, the chemo-marker also constitutes a biomarker of the extract.

We demonstrated that the *Lythrum salicaria* extract could be used as an active ingredient with beneficial effects for the skin homeostasis with a pro-differentiating effect and a global protecting or reinforcement action. This effect was characterized by the generation of well-structured epidermis and by maintaining the skin protective functions for the body.

Lythrum salicaria L. may now be considered as a new great source of active ingredients with protecting and anti-aging effects for skin.

Acknowledgments: This study on *Lythrum salicaria* was part of the Project ECOSMETOCENTRE certified by the competitiveness cluster DREAM in the Région Centre-Val de Loire in France. It was funded by the 'Ministère de l'Economie et des Finances' in France.

Author Contributions: Franck Himbert, Philippe Bernard and François-Xavier Bernard conceived and designed the experiments; Glorianne Jouravel and Samuel Guénin performed the experiments, Franck Himbert, Philippe Bernard and François-Xavier Bernard and Samuel Guénin analyzed the data; Glorianne Jouravel and Samuel Guénin wrote the paper; Claire Elfakir contributed to the elaboration of the final version of the paper by giving corrections and suggestions for the paper.

Conflicts of Interest: The authors declare no conflict of interest. The founding sponsors had no role in the design of the study; in the collection, analyses, or interpretation of data; in the writing of the manuscript, and in the decision to publish the results.

References

1. Piwowarski, J.P.; Granica, S.; Kiss, A.K. *Lythrum salicaria* L.—Underestimated medicinal plant from European traditional medicine. A review. *J. Ethnopharmacol.* **2015**, *170*, 226–250. [[CrossRef](#)] [[PubMed](#)]
2. Manayi, A.; Khanavi, M.; Saiednia, S.; Hadjiakhoondi, A.; Azizi, E.; Mahmoodpour, M.; Vafi, F.; Siavashi, F.; Malmir, M. Biological activity and microscopic characterization of *Lythrum salicaria* L. *Daru J. Pharm. Sci.* **2013**, *21*, 61. [[CrossRef](#)] [[PubMed](#)]
3. Piwowarski, J.P.; Kiss, A.K. C-glycosidic Ellagitannins from *Lythri herba* (European Pharmacopoeia): Chromatographic Profile and Structure Determination. *Phytochem. Anal.* **2013**, *24*, 336–348. [[CrossRef](#)] [[PubMed](#)]
4. Mukherjee, P.K.; Maity, N.; Nema, N.K.; Sarkar, B.K. Bioactive compounds from natural resources against skin aging. *Phytomedicine* **2011**, *19*, 64–73. [[CrossRef](#)] [[PubMed](#)]
5. Allemann, I.B.; Baumann, L. Botanicals in skin care products. *Int. J. Dermatol.* **2009**, *48*, 923–934. [[CrossRef](#)] [[PubMed](#)]
6. Simpson, C.L.; Patel, D.M.; Green, K.J. Deconstructing the skin: Cytoarchitectural determinants of epidermal morphogenesis. *Nat. Rev. Mol. Cell Biol.* **2011**, *12*, 565–580. [[CrossRef](#)] [[PubMed](#)]
7. Candi, E.; Schmidt, R.; Melino, G. The cornified envelope: A model of cell death in the skin. *Nat. Rev. Mol. Cell Biol.* **2005**, *6*, 328–340. [[CrossRef](#)] [[PubMed](#)]
8. Holleran, W.M.; Takagi, Y.; Menon, G.K.; Legler, G.; Feingold, K.R.; Elias, P.M. Processing of epidermal glucosylceramides is required for optimal mammalian cutaneous permeability barrier function. *J. Clin. Investig.* **1993**, *91*, 1656–1664. [[CrossRef](#)] [[PubMed](#)]
9. Rawlings, A.V. Trends in stratum corneum research and the management of dry skin conditions. *Int. J. Cosmet. Sci.* **2003**, *25*, 63–95. [[CrossRef](#)] [[PubMed](#)]
10. Fuchs, E.; Raghavan, S. Getting under the skin of epidermal morphogenesis. *Nat. Rev. Genet.* **2002**, *3*, 199–209. [[CrossRef](#)] [[PubMed](#)]
11. Gibbs, S.; Ponc, M. Intrinsic regulation of differentiation markers in human epidermis, hard palate and buccal mucosa. *Arch. Oral Biol.* **2000**, *45*, 149–158. [[CrossRef](#)]
12. Marte, B.; Finkelstein, J.; Anson, L. Skin Biology. *Nature* **2007**, *445*, 833. [[CrossRef](#)]
13. Rinnerthaler, M.; Streubel, M.K.; Bischof, J.; Richter, K. Skin aging, gene expression and calcium. *Exp. Gerontol.* **2015**, *68*, 59–65. [[CrossRef](#)] [[PubMed](#)]
14. Baumann, L.; Woolery-Lloyd, H.; Friedman, A. Natural Ingredients in Cosmetic Dermatology. *J. Drugs Dermatol.* **2009**, *8*, s5–s9. [[PubMed](#)]
15. Rabeony, H.; Petit-Paris, I.; Garnier, J.; Barrault, C.; Pedretti, N.; Guilloteau, K.; Jegou, J.-F.; Guillet, G.; Huguier, V.; Lecron, J.-C.; et al. Inhibition of Keratinocyte Differentiation by the Synergistic Effect of IL-17A, IL-22, IL-1 α , TNF α and Oncostatin M. *PLoS ONE* **2014**, *9*, e101937. [[CrossRef](#)] [[PubMed](#)]
16. Guenou, H.; Nissan, X.; Larcher, F.; Feteira, J.; Lemaitre, G.; Saidani, M.; Del Rio, M.; Barrault, C.C.; Bernard, F.-X.; Peschanski, M.; et al. Human embryonic stem-cell derivatives for full reconstruction of the pluristratified epidermis: A preclinical study. *Lancet* **2009**, *374*, 1745–1753. [[CrossRef](#)]
17. Rauha, J.-P.; Wolfender, J.-L.; Vuorela, H. Characterization of the polyphenolic composition of purple loosestrife (*Lythrum salicaria*). *Z. Für Naturforschung C* **2000**, *56c*, 13–20. [[CrossRef](#)]
18. Nonaka, G.; Nishioka, I. Tannins and Related Compounds. XCVII. Structure revision of C-glycosidic ellagitannins, Castalagin, Vescalagin, Casuarinin and Stachyurin, and related hydrolyzable tannins. *Chem. Pharm. Bull. (Tokyo)* **1990**, *38*, 2151–2156. [[CrossRef](#)]
19. Tanaka, T.; Kouno, I. Four new C-glycosidic ellagitannins, Castacrenins D-G, from Japanese Chestnut Wood (*Castanea crenata* SIEB. et ZUCC.). *Chem. Pharm. Bull. (Tokyo)* **1997**, *45*, 1751–1755. [[CrossRef](#)]
20. Lee, W. J.; Park, K. H.; Cha, H. W.; Sohn, M. Y.; Park, K. D.; Lee, S.-J.; Kim, D. W. The Expression of Involucrin, Loricrin, and Filaggrin in Cultured Sebocytes. *Ann. Dermatol.* **2014**, *26*, 134. [[CrossRef](#)] [[PubMed](#)]
21. Vičanová, J.; Boelsma, E.; Mommaas, A.M.; Kempenaar, J.A.; Forslind, B.; Pallon, J.; Egelrud, T.; Koerten, H.K.; Ponc, M. Normalization of epidermal calcium distribution profile in reconstructed human epidermis is related to improvement of terminal differentiation and stratum corneum barrier formation. *J. Investig. Dermatol.* **1998**, *111*, 97–106. [[CrossRef](#)] [[PubMed](#)]

22. Zhuang, Y.; Lyga, J. Inflammaging in Skin and other Tissues - The Roles of Complement System and Macrophage. *Inflamm. Allergy - Drug Targets* **2014**, *13*, 153–161. [[CrossRef](#)] [[PubMed](#)]
23. Philips, N.; Auler, S.; Hugo, R.; Gonzalez, S. Beneficial Regulation of Matrix Metalloproteinases for Skin Health. *Enzyme Res.* **2011**, *2011*, 1–4. [[CrossRef](#)] [[PubMed](#)]



© 2017 by the authors. Licensee MDPI, Basel, Switzerland. This article is an open access article distributed under the terms and conditions of the Creative Commons Attribution (CC BY) license (<http://creativecommons.org/licenses/by/4.0/>).